EPJ B
Condensed Matter and Complex Systems
EPJ.org
your physics journal

Eur. Phys. J. B (2016) 89: 83 DOI: 10.1140/epjb/e2016-60965-1

Stochastic resonance phenomenon in Monte Carlo simulations of silver adsorbed on gold

María Cecilia Gimenez

edp sciences
Società Italiana di Fisica
Springer

Eur. Phys. J. B (2016) 89: 83
DOI: 10.1140/epjb/e2016-60965-1

THE EUROPEAN PHYSICAL JOURNAL B

Regular Article

Stochastic resonance phenomenon in Monte Carlo simulations of silver adsorbed on gold

María Cecilia Gimenez[a]

IFEG, Conicet, FaMAF, Universidad Nacional de Cordoba, 5000 Cordoba, Argentina

Received 15 December 2015 / Received in final form 10 February 2016
Published online 28 March 2016 –

Abstract. The possibility of observing the stochastic resonance phenomenon was analyzed by means of Monte Carlo simulations of silver adsorbed on 100 gold surfaces. The coverage degree was studied as a function of the periodical variation of the chemical potential. The signal-noise relationship was studied as a function of the amplitude and frequency of chemical potential and temperature. When this value is plotted as a function of temperature, a maximum is found, indicating the possible presence of stochastic resonance.

1 Introduction

Research on electrochemical deposition of a metal M onto the surface of a foreign metal S should provide a better understanding of the fundamental aspects of metal deposition [1–8]. When this takes place at potentials more positive than those predicted from the Nernst equation, the process is called underpotential deposition (upd) [2–5]. This phenomenon has previously been studied by means of first principle calculations [9] and the embedded atom method (EAM) [10,11].

It is the purpose of this work to analyze the stochastic resonance phenomenon [12] occurring when a periodically variable chemical potential is applied to the adsorption of Ag atoms on a Au(100) surface in order to alternatively adsorb and desorb the silver monolayer.

As they provide a realistic interaction of the metallic binding, EAM potentials [13–15] are employed to describe atom-atom interaction. Using the Monte Carlo method within a lattice model allows us to deal with systems having a reasonably large number of particles.

We have previously studied the Ag on Au(100) system, as well as other related ones by means of Monte Carlo [16–18] and dynamic Monte Carlo simulations [19,20]. Besides, we have studied the application of a periodically varying chemical potential in order to study dynamic phase transitions [21].

Stochastic resonance (SR) refers to a situation where the addition of random noise improves the response of the system to a periodical signal [12,22]. The stochastic resonance phenomenon was originally studied in the early 80's by two groups, in Rome [23] and Brussels [24]. It arose at a new idea to explain the almost periodic occurrence of the ice ages. After that, the idea of stochastic resonance has spread well beyond physics and left its fingerprints in many other scientific disciplines, like biology [25].

As some particular examples, some experimental studies of the stochastic resonance phenomenon were performed for the case of active-passive transition of iron in sulfuric acid [26] and for a three-electrode electrochemical cell configured for studying the potentiostatic electrodissolution of iron in a solution of copper sulfate and sulfuric acid [27]. The latter study demonstrates that stochastic resonance occurs for aperiodic subthreshold signals in electrochemical systems.

In the present study, we will focus on the signal-to-noise relationship (for the Fourier transform) as a function of the temperature, amplitude and frequency of the chemical potential. Similar studies of the stochastic resonance phenomenon have previously been done in the context of a different system: opinion models related to sociophysics [28,29]. In the case of opinion models we have two possible states for each opinion (+1 or −1), an oscillating external field that plays the role of propaganda and a "social temperature". That system bears several similarities with the present one, where the occupation state of an absorption site would be equivalent to the two opinion states, the chemical potential would play the role of propaganda and the traditional temperature would be analogous to "social temperature".

This paper is organized as follows: the model and simulation method are introduced in Section 2, the main results and discussion are presented in Section 3, and the conclusions are given in Section 4.

2 Model and simulation method

2.1 Lattice model

Lattice models allow dealing with a large number of particles at a relatively low computational cost. For that reason they are widely used in computer simulations to study adsorption processes on surfaces. To assume that particle

[a] e-mail: ceciliagim@gmail.com

adsorption can only occur at definite sites is a good approximation for some systems. Such is the case of Ag on Au(100), where there is no crystallographic misfit.

For the purpose of this study, lattice model was employed to represent the square (100) gold surface lattice in a Grand Canonical Monte Carlo simulation. Square lattices of size (100×100) with periodical boundary conditions are used here to represent the surface. Each lattice node constitutes an adsorption site for a silver atom.

2.2 Energy calculation

To calculate the adsorption energies for silver particles the Embedded Atom Method (EAM) was used [13–15]. As this method takes into account many-body effects, it represents metallic bonding better than a pair potential does. The total energy of the system is calculated as the sum of the energy of individual particles. Each of these energies is in turn the sum of an embedding (attractive) energy and a repulsive contribution which arises from the interaction between ion cores. The EAM contains parameters which were fitted to reproduce experimental data, such as elastic constants, enthalpies of binary alloys dissolution, lattice constants, and sublimation heats.

Application of the EAM within a lattice model has been described in detail in previous works [16,17].

2.3 Grand canonical Monte Carlo

One of the most appealing features of Grand Canonical Monte Carlo ($\mu VT/MC$) is that, as in many experimental situations, the chemical potential μ is one of the independent variables.

Such is the case of low-sweep rate voltammetry, an electrochemical technique where the electrode potential can be used to control the chemical potential of species at the metal/solution interface. At the solid-vacuum interface, the chemical potential is related to the vapor pressure of the gas in equilibrium with the surface.

Our 2D system is characterized by a square lattice with M adsorption sites. We labeled each adsorption site either 0 or 2, depending on whether it is empty or occupied by one adsorbate atom, respectively.

Following the procedure proposed by Metropolis and coworkers [30], the acceptance probability for a transition from state $\overrightarrow{n}$ to $\overrightarrow{n}'$ is defined as:

$$W_{\overrightarrow{n}\to\overrightarrow{n}'} = \min\left(1, \exp^{-\left(\frac{\Delta E-\mu\Delta N}{k_b T}\right)}\right) \tag{1}$$

where μ is the chemical potential, $\Delta N = +1$ if a particle is adsorbed or -1 if a particle is desorbed, ΔE denotes the adsorption energy of the particle at a particular site with a particular environment taking into account first, second and third neighbors (see Ref. [16] for technical details), k_b is the Boltzmann constant, and T is the temperature. This probability is related with the Boltzmann distribution in the Grand Canonical ensemble and it can be demonstrated that it leads to a sampling of states in the configuration space according to that distribution, following the Metropolis algorithm [31].

Our $\mu VT/MC$ simulation allows for two types of events:

1. adsorption of an adsorbate atom onto a randomly-selected lattice site;
2. desorption of an adsorbate atom from an occupied lattice site selected at random.

Within this procedure, the relevant thermodynamic property to be obtained is the coverage degree as a function of the chemical potential μ, where the instantaneous value, $\theta(\mu)_{Ads}$, is defined as follows:

$$\theta(\mu)_{Ads} = \frac{N_{Ads}}{M} \tag{2}$$

where N_{Ads} is the number of adsorbate atoms and M denotes the total number of sites.

2.4 Algorithm employed for the calculation of energy differences

One of the main advantages of the lattice model is that it fixes the distances between the adsorption nodes, thus reducing to a discrete set the possible difference of energy values the system can take. Furthermore, a very important simplifying assumption can be made for obtaining ΔE. The point is to consider the adsorption (desorption) of a particle at a node immersed in a certain environment, that includes first, second and third neighbors giving a total of 13 sites, including the central atom. Then, the adsorption energy for all the possible configurations of the environment of the central atom can be calculated before performing the simulation. With this method all the adsorption energies of an atom are tabulated, so that during the MC simulation the most expensive numerical operations are reduced to the reconstruction of the number I that characterizes the configuration surrounding the particle on the adsorption node. Computationally speaking, I is nothing but the index of the array in which the energy is stored. See references [16,17] for more technical details.

2.5 Periodic variation of the chemical potential

The chemical potential μ is varied periodically according to:

$$\mu = \mu_0 + A \times \sin(\omega t), \tag{3}$$

where μ_0 denotes the chemical potential at which transition occurs (between covered and uncovered surface), A is the amplitude of oscillation (we take $0 \leq A \leq 1$) and $\omega = 2\pi/P$ (P = period) is the angular frequency. The time evolution, t, is taken in this case in units of Monte Carlo Steps (MCS).

2.6 Signal-noise relationship

In order to study resonant effects, we have calculated the Fourier transform of θ as a function of time.

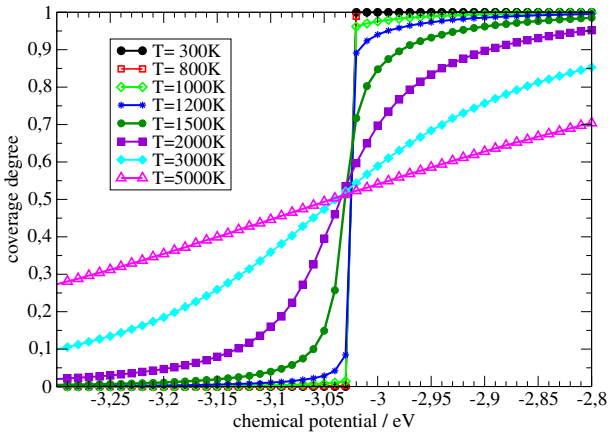

Fig. 1. Coverage degree, θ as a function of the chemical potential, μ (in eV) at different temperatures ($T = 300$ K, 800 K, 1000 K, 1200 K, 1500 K, 2000 K, 3000 K and 5000 K).

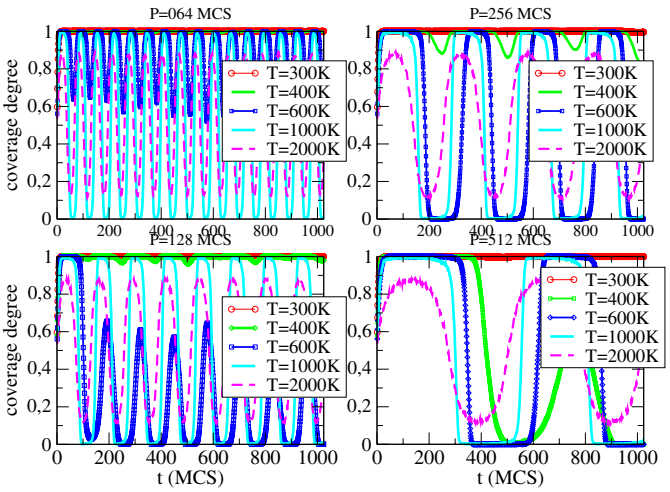

Fig. 2. Response of the coverage degree to a periodical variation of the chemical potential, for an oscillation amplitude of $A = 0.10$, period values $P = 64$ MCS, 128 MCS, 256 MCS and 512 MCS, and several temperatures, as indicated.

Signal-to-noise ratio (SNR) is a measure that compares the level of a desired signal to the level of background noise. It is defined as the ratio of signal power to noise power. A ratio higher than 1 : 1 indicates more signal than noise.

Thus, signal-to-noise ratio is defined as the ratio of the power of a signal (meaningful information) to the power of background noise (unwanted signal):

$$SNR = \frac{P_{signal}}{P_{noise}}, \tag{4}$$

where P is the average power in the Fourier space. P_{signal} denotes the maximum value of the signal and P_{noise} is the value of the background, averaged before and after the signal peak.

For our current purpose, it was calculated as:

$$SNR = \frac{(h-n)}{n} \tag{5}$$

where h is the height of the peak at that frequency and n denotes the height of the noise in the ground of that region, calculated as the average value after and before the maximum.

3 Results and discussion

Figure 1 shows isotherms of the coverage degree as a function of the chemical potential for the adsorption of Ag on Au(100) at different temperatures. At low temperatures, an abrupt step in the coverage degree can be observed for a certain value of the chemical potential, indicating the presence of a first-order phase transition. At high temperatures, interaction between adjacent adatoms becomes less important and the shape of the isotherms is similar to Langmuir approximations. The value of the chemical potential at which transition occurs is around $\mu_0 = -3.02$ eV, which for the purposes of this study will be taken as the reference value of μ_0 to analyze periodical variations.

The present model is similar to the Ising model in the sense that there are lateral interactions between adsorbed particles. In a previous work [18], we have taken into account lateral interaction between adsorbing particles as a pair-potential and only between nearest neighbors. It is well known that in this case the critical temperature for $\theta = 0.5$ can be estimated as [32]:

$$T_C = \frac{J}{2k_B \ln(\sqrt{2}-1)} \tag{6}$$

where J is the lateral interaction between adsorbing particles. Taking into account the values for J employed in that work, the estimated critical temperature was $T_C = 1843$ K for the system Ag/Au(100).

Nevertheless, in the present work we are not dealing with pair-potential intereactions, but as the EAM was employed, there are some non-linearities, especially in the attractive terms of the energy calculation. If we take into account the energies corresponding to the adsorption configurations presented in a previous work [17], the estimated difference between the adsorption energy with all neighboring sites occupied by silver atoms and the adsorption energy with all neighboring sites unoccupied is about -0.778 eV. If we divide that number by 4 (in order to consider first-neighbor interactions), the estimated value for J is now about -0.1945 eV, given an estimated value of 1280 K for the critical temperature.

The periodical variation of the chemical potential was studied. Several periods ($P = 16$, 32, 64, 128, 256 and 512), amplitudes ($A = 0.05$, 0.10, 0.15, 0.20, 0.50 and 0.80) and temperatures (T) were employed in the simulations.

Figure 2 shows time evolution for four of the employed periods ($P = 64$, 128, 256 and 512) and several temperatures, in the case of amplitude $A = 0.10$. In this case, for low temperatures, the coverage does not follow the external signal, especially at low periods. For temperature

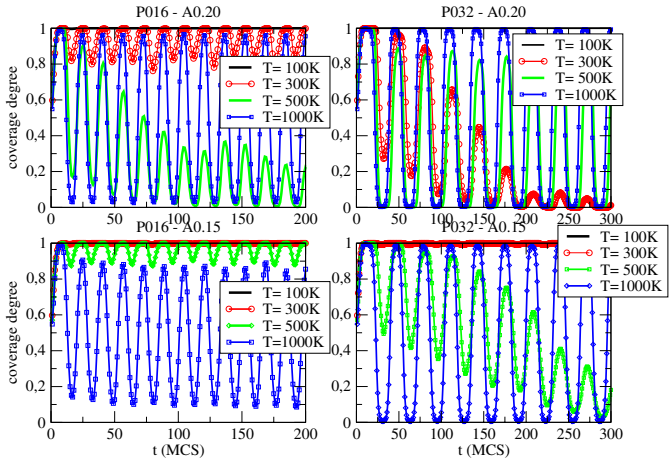

Fig. 3. Response of the coverage degree to a periodical variation of the chemical potential, for oscillation amplitudes of $A = 0.15$ and 0.20 and periods $P = 16$ MCS and $P = 32$ MCS, for several temperatures, as indicated.

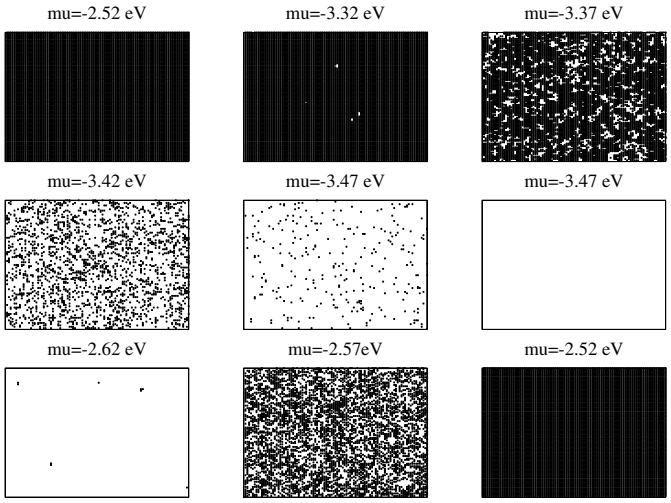

Fig. 4. Frames showing the microscopic behaviour of the coverage degree at different chemical potentials along one cycle, for an oscillation amplitude of $A = 0.50$, a period $P = 64$ and a temperature $T = 100$ K.

$T = 300$ K, θ remains constant at value 1 and the same occurs for $T = 400$ K at low periods. At high periods, θ shows some irregular variation for $T = 400$ K, while for $T = 600$ K and 1000 K, it follows the signal perfectly, oscillating between 0 and 1. For $T = 2000$ K, the coverage follows the signal too, but the amplitude is less than 1.

Figure 3 depicts time evolution for two of the employed periods ($P = 16$ and 32) and several temperatures, in the case of amplitudes $A = 0.15$ and $A = 0.20$. It can be seen that for low temperatures the coverage degree does not follow the signal; for intermediate (but still low) temperatures, the coverage degree follows partially the chemical potential, oscillating around one of the extremes, and for high temperatures, θ perfectly follows the signal.

In the case of amplitude $A = 0.50$ or higher (not shown), the coverage degree always follows the external signal perfectly, oscillating between 0 and 1.

Figure 4 shows frames describing the microscopic behavior of the silver atoms on the surface while they are changing from total coverage to desorption and vice versa during one cycle, in the case of $A = 0.50$, $P = 64$ and $T = 100$ K. It can be noticed that the transformation occurs mainly through a multidroplet process, which involves the formation of several nuclei of one phase inside the other one. This fact was observed for all the cases studied. It must be noticed that the transition does not take place in the cases of low amplitude ($A = 0.2$) and low temperatures. This fact calls into question whether or not we are in the presence of stochastic resonance. For a detailed discussion of this phenomenon see references [33–35].

The value of τ (time required to change the coverage degree from 0 to 1 or vice versa) was calculated by averaging over 100 cycles of change of chemical potential from $\mu_0 - A$ to $\mu_0 + A$ and vice versa, for some typical cases. The results are shown in Figure 5 as a function of temperature, for several amplitude values. The case of passage from $\theta = 0$ to $\theta = 1$ is shown separately from the case of passage from $\theta = 1$ to $\theta = 0$ because the system is not

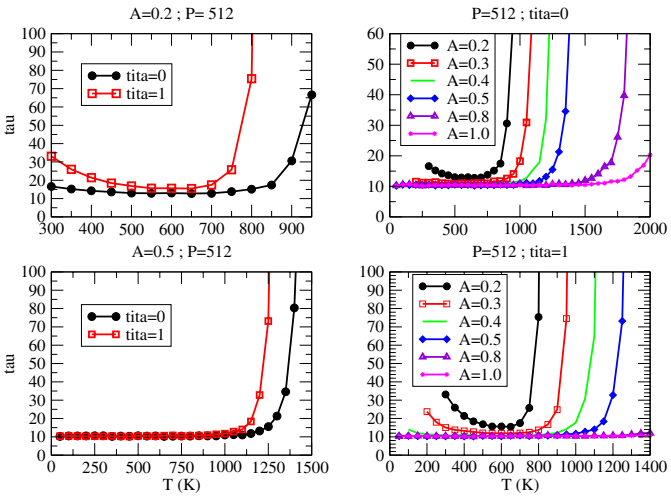

Fig. 5. Value of τ (time required to change the coverage degree from one extreme to the other, under a sudden change of the chemical potential) as a function of the temperature. Left: comparison between the τ for the passage from $\theta = 0$ to $\theta = 1$ (open red squares) and the passage from $\theta = 1$ to $\theta = 0$ (filled black circles), for two amplitudes ($A = 0.2$ and $A = 0.5$). Right: comparison between several amplitudes, for the kinds of passage (from $\theta = 1$ to $\theta = 0$ and from $\theta = 0$ to $\theta = 1$).

symmetrical and the two τ values are not equivalent. In most cases, the value of τ remains more or less constant until a certain temperature at which it rises abruptly. This can be explained because it takes a lot of time to reach the value 0 or 1 because at high temperatures the transition is slower and it spends more time at intermediate values. For $A = 0.2$ the general value is higher, but for the rest of amplitudes, it is approximately in the order of $\tau \simeq 10$ MCS, at not very high temperatures.

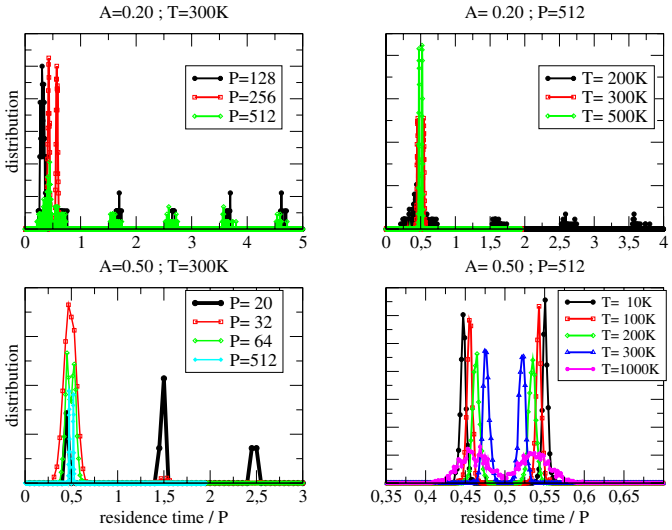

Fig. 6. Residence time distribution for different combinations of amplitude (in eV), period, P (in MCS) and temperatures (in K), as indicated. The main peak is always at $0.5P$ and in some cases there are other subpeaks at $(n + 1/2)P$. It can also be observed the splitting of the main peak in two parts, correspondig to the adsorption and the desorption processes, because they are not exactly symmetrical.

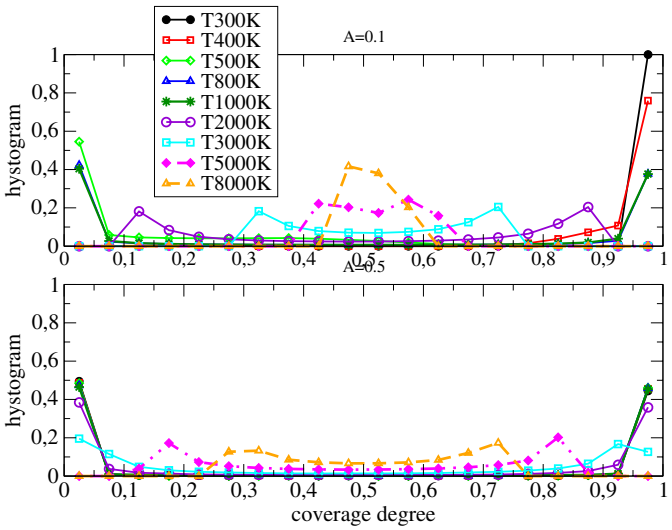

Fig. 7. Distribution histograms of coverage degree, for oscillation amplitudes of the chemical potential $A = 0.1$ and $A = 0.5$, period $P = 256$ MCS and several temperatures, as indicated.

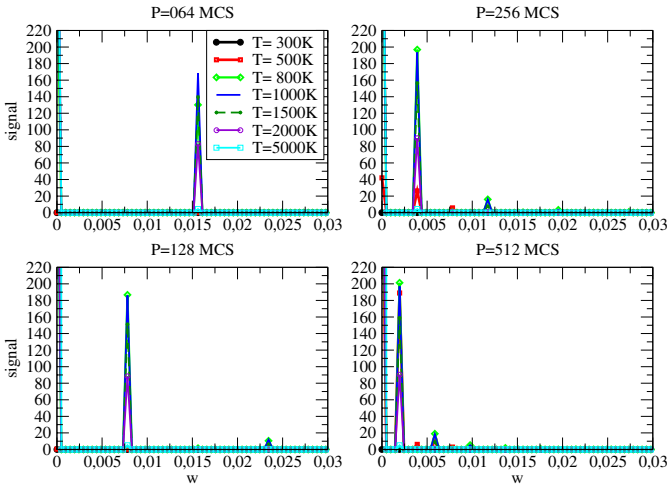

Fig. 8. Fourier transform of the coverage degree as a function of the oscilating chemical potential for amplitude $A = 0.10$, periods $P = 64$ MCS, $P = 128$ MCS, $P = 256$ MCS and $P = 512$ MCS, and several temperatures, as indicated. The main peak corresponds to the oscilation period of the chemical potential.

According to reference [12], the relationship between τ and the period of the oscillation must be about $2 \times \tau = P$ in order for stochastic resonance to be observed.

In order to estimate residence time distributions, simulations of 1000 cycles were performed. The residence time was defined as the number of Monte Carlo steps needed to reach $\theta = 1$ if starting $\theta = 0$ and vice versa. The distribution of residence times for different conditions is shown in Figure 6. In the left side, different periods are compared for the cases of amplitudes $A = 0.2$ and $A = 0.5$ and $T = 300$ K. In most cases the mean peak is located at $rt/P = 0.5$, but for $A = 0.2$ and low periods of $A = 0.5$, there are other peaks at $rt/P = 1.5, 2.5$, etc. In the right side of the figure, different temperatures are compared, for $A = 0.2$ and $A = 0.5$ and period $P = 512$.

One of the main characteristics of all the residence time distributions is that there are two peaks instead of one. The first one corresponds to the passage from $\theta = 1$ to $\theta = 0$ and the second one to the opposite case. This is due to the non-symmetry of the system for the covering and the desorption process.

Figure 7 depicts the distribution of θ (probability of obtaining each particular value of θ) for nine different temperatures and $P = 256$ in the case of amplitudes $A = 0.1$ and $A = 0.5$, averaged over 512 simulations. For each simulation, the average was taken over the last 1024 temporal steps, that is in the stationary regime (after 1024 equilibration steps). For the case of $A = 0.1$, at low temperatures ($T = 300$ K and $T = 400$ K), θ is concentrated at value 1 and it becomes distributed between the values 0 and 1 at intermediate temperatures. As temperature increases, θ becomes more or less symmetrically distributed at both sides of the centre, approaching the middle point ($\theta = 0.5$) at very high temperatures. For amplitude $A = 0.5$, at temperatures lower than $T = 2000$ K, θ is symmetrically distributed between the values 0 and 1. As temperature increases $\theta =$ distribution shifts towards the centre, but misses the center position.

In order to analyze the response of θ to the external periodical variation of μ, the Fourier transform was studied. The average was taken over 10 simulations, each one of 2048 steps (after some equilibration period) and the signal is plotted in Figure 8 for the case of amplitude $A = 0.10$, four of the studied periods ($P = 64$, $P = 128$, $P = 256$ and $P = 512$) and several temperatures. As it can be noticed, the main peak is located at $1/P$ in the Fourier

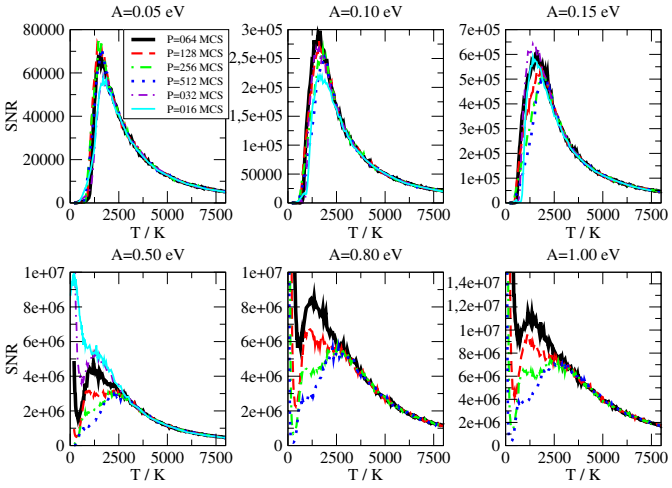

Fig. 9. SNR as a function of temperature, for different periods and amplitudes, as indicated. For amplitudes $A = 0.05$ eV, $A = 0.10$ eV and $A = 0.15$ eV, there is a unique maximum, for a certain temperature, and the shape of the curve is approximately independent of the period. For higher amplitudes ($A = 0.50$ eV, $A = 0.80$ eV and $A = 1.00$ eV) the initial values are very high, then the curves reach a minimum, and then increases again until a maximum. In these cases the dependence with the period is stronger.

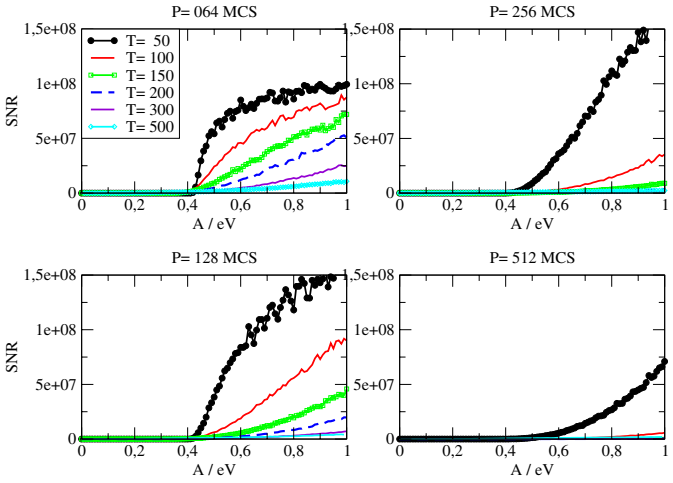

Fig. 10. SNR as a function of amplitude, for periods $P = 64$, $P = 128$, $P = 256$ and $P = 512$, and relatively low temperatures ($T = 50$ K, $T = 100$ K, $T = 150$ K, $T = 200$ K, $T = 300$ K, $T = 500$ K). The initial value of SNR is zero, but, from a certain threshold, it starts to increase.

coordinate space. This peak is employed to calculate *SNR* (signal-noise relationship), by the equations described in Section 2.6. The signal at zero in the Fourier transform corresponds to the background noise, where no frequency is present at all. In practice, we calculate de height h of the peak and the background (n = noise) as the average value of the two adjacent points. Then, *SNR* value is estimated as $SNR = (h - n)/n$.

Figure 9 shows *SNR* as a function of temperature, for different frequencies and amplitudes. As it can be seen, for low amplitudes ($A = 0.05$, $A = 0.10$ and $A = 0.15$), the curves are similar for the different frequencies. They are zero for low temperatures, then they abruptly increase presenting a maximum value, after that, they decrease exponentially. For higher amplitude values (in this case $A = 0.50$, $A = 0.80$ and $A = 1.00$), *SNR* starts at very high values, then showing a minimum and increasing again up to a maximum value. The position of the peaks depends on frequency and it moves towards higher values of T and lower values of *SNR* as the period increases. After that, the curves decrease in all cases and match each other for the different frequencies.

The maximum at the beginning in the case of large amplitudes implies that the coverage perfectly follows the external chemical potential even for low temperatures. That is not an example of stochastic resonance, because the response does not need the noise in order to be coupled to the external signal. In this case, the coverage oscilates near $\theta = 1$ or near $\theta = 0$ following the signal but without passing from one state to the other one. Stochastic resonance is due to the optimal relationship between the signal and the noise. Thus, the peak corresponding to that phenomenon is the second one.

It can be noticed that, for most cases, the maximum is located at temperatures higher than the critical one. This fact also calls into question whether or not we are in the presence of the stochastic resonance phenomenon. The peak is around the critical temperature or less in the cases of large amplitudes and low periods, indicating that for these cases we can effectively talk about stochastic resonance.

Figures 10 and 11 show the variation of *SNR* with amplitude, for different temperatures. Low and high temperatures can be observed in Figures 10 and 11, respectively. It can be noticed that for low temperatures the response is zero below certain threshold amplitude. On the other hand, for high temperatures, the value of *SNR* increases nearly linearly with A. At low temperatures and large amplitudes, *SNR* value is very high.

The threshold value of the amplitude at which *SNR* is no longer null was calculated for each temperature and frequency. Figure 12 shows threshold amplitude as a function of temperature for the four frequencies studied. In most cases, the threshold starts near $A = 0.4$ and then decreases until reaching zero from a certain temperature value.

Finally, Figure 13 shows the signal-noise relationship as a function of the period, for different amplitudes and temperatures. For these particular cases, a maximum can be observed for a certain value of P, which may indicante that we are in the presence of stochastic resonance.

4 Summary and discussion

The response of the coverage degree of silver adsorption on a gold surface to a periodical chemical potential was studied by means of Grand Canonical Monte Carlo simulations.

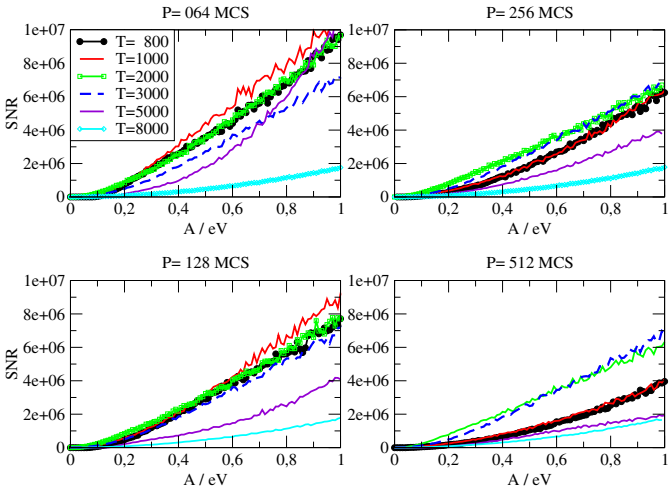

Fig. 11. *SNR* as a function of amplitude, for periods $P = 64$, $P = 128$, $P = 256$ and $P = 512$, and relatively high temperatures ($T = 800$ K, $T = 1000$ K, $T = 2000$ K, $T = 3000$ K, $T = 5000$ K, $T = 8000$ K). The initial value of *SNR* is zero and it increases more or less linearly.

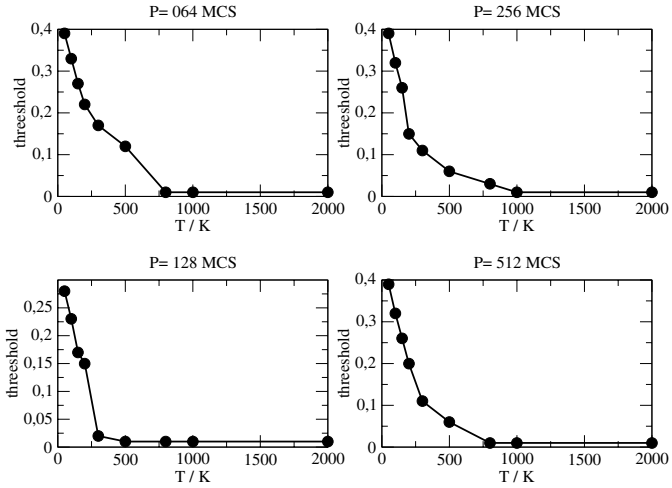

Fig. 12. Amplitude threshold for the observation of *SNR* as a function of temperature for $P = 64$ MCS, $P = 128$ MCS, $P = 256$ MCS and $P = 512$ MCS.

In general, the response of the signal coverage follows the chemical potential, except for small amplitudes and low temperatures. In most cases the value of τ (mean time to change phase) is in the order of 20 MCS. In graphs of *SNR* as a function of temperature, there is generally a maximum, which indicates that we are probably in the presence of stochastic resonance. The peak is near the critical temperature in the case of large amplitudes and low periods. For the other cases the temperature corresponding to the peaks is higher than T_C, indicating that it may not be a case of stochastic resonance, but we can observe dynamic phase transitions. At low temperatures, a threshold value of amplitude is observed for the *SNR* response. The curves of *SNR* as a function of the period show a maximum for certain combinations of amplitudes and temperatures.

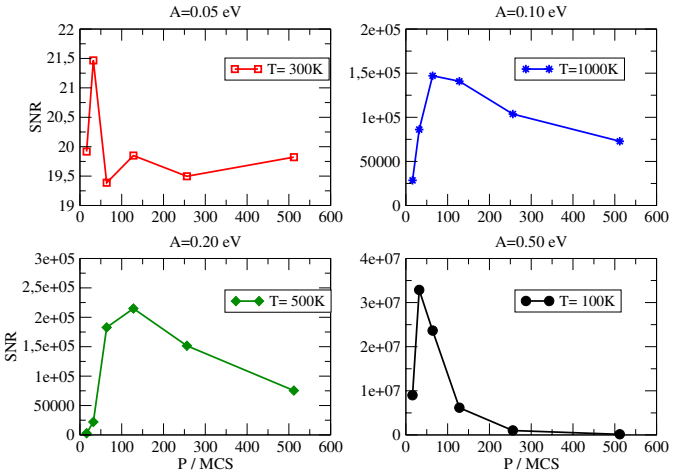

Fig. 13. *SNR* as a function of period, for different combinations of amplitudes and temperatures ($A = 0.05$ eV and $T = 300$ K; $A = 0.10$ eV and $T = 1000$ K; $A = 0.20$ eV and $T = 500$ K; $A = 0.50$ eV and $T = 100$ K). For these combinations of parameters, a maximum can be observed.

The behavior of this system was found to be qualitatively analogous to an opinion model with two possible opinion values and external propaganda. The two possible opinion values are equivalent to the two states of each adsorption site (occupied or empty) while the periodically varying external propaganda is the analogue of the chemical potential.

Some related experimental studies can be suggested. One possibility would be to carry out the periodic variation of the chemical potentials in an electrochemical cell adapted for the study of underpotential deposition of Ag on Au(100). This can be done either by means of linear sweeps, alternatively changing from one direction to the oppossite or by discrete steps of chemical potential, oscillating periodically between two values (one corresponding to the coverage of silver and the other with no coverage associated). However, the experimental realization of these studies, present some difficulties due to the range of parameters employed. The main advantage of computer simulations is that it is possible to explore ranges of parameters that are difficult to achieve experimentally. In this particular case, the amplitudes taking into account are very high and in real experiments it would comprisses a lot of adittional processes. Real impedance experiments, for instance, involve amplitudes of oscilation lower than 0.01 eV, but in the present numerical calculations, the amplitudes must be higher in order to detect some response. On the other hand, in impedance experiments, a very large range of frequencies are explored, but here we have the limitation of taking values equal to powers of two, due to the numerical algorithm for the fourier transform. Also, the temperatures involved in this work are very high for real systems. Instead of impedance, STM studies can be realized, in order to detect the coverage and decoverage processes. Some future work will be oriented in that direction.

M.C. Gimenez acknowledges National Council of Scientific and Technological Research of Argentina (Conicet); Secyt UNC, for finantial support; CONICET-PIP 11220110100992 y Program BID (PICT 2012-2324), for computational tools. Fruitfull discussions with Antonio J. Ramirez-Pastor, Jorge A. Revelli and Lucía Avalle are gratefully acknowledged. Language assistance by Karina Plasencia is gratefully acknowledged.

References

1. D.M. Kolb, in *Advances in Electrochemistry and Electrochemical Engineering*, edited by H. Gerischer, C.W. Tobias (Wiley, New York, 1978), Vol. 11, p. 125
2. D.M. Kolb, M. Przasnyski, H. Gerischer, J. Electroanal. Chem. **54**, 25 (1974)
3. S. Trasatti, Z. Phys. Chem. **98**, 75 (1975)
4. L. Blum, D.A. Huckaby, M. Legault, Electrochim. Acta **41**, 2201 (1996)
5. K. Jutttner, G. Staikov, W.J. Lorenz, E. Schmidt, J. Electroanal. Chem. **80**, 67 (1977)
6. E.P.M. Leiva, in *Current Topics in Electrochemistry* (Council of Scientific Information, Trivandrum, 1993), Vol. 2, p. 269
7. E.P.M. Leiva, Electrochim. Acta **41**, 2185 (1996)
8. E. Budevski, G. Staikov, W.J. Lorenz, *Electrochemical Phase Formation and Growth* (VCH, Weinheim, 1996)
9. C. Sánchez, E.P.M. Leiva, J. Kohanoff, Langmuir **17**, 2219 (2001)
10. C.G. Sánchez, M.G. Del Pópolo, E.P.M. Leiva, Surf. Sci. **421**, 59 (1999)
11. M.I. Rojas, C.G. Sánchez, M.G. Del Pópolo, E.P.M. Leiva, Surf. Sci. **453**, 225 (2000)
12. L. Gammaitoni, P. Hänggi, P. Jung, F. Marchesoni, Rev. Mod. Phys. **70**, 223 (1998)
13. S.M. Foiles, M.I. Baskes, M.S. Daw, Phys. Rev. B **33**, 7983 (1986)
14. E. Clementi, C. Roetti, At. Data Nucl. Data Tables **14**, 177 (1974)
15. A.D. McLean, R.S. McLean, At. Data Nucl. Data Tables **26**, 197 (1981)
16. M.C. Giménez, M.G. Del Pópolo, E.P.M. Leiva, Electrochim. Acta **45**, 699 (1999)
17. M.C. Gimenez, E.P.M. Leiva, Langmuir **19**, 10538 (2003)
18. M.C. Gimenez, A.J. Ramirez-Pastor, E.P.M. Leiva, Surf. Sci. **600**, 4741 (2006)
19. M.C. Giménez, M.G. Del Pópolo, E.P.M. Leiva, S.G. García, D.R. Salinas, C.E. Mayer, W.J. Lorenz, J. Electrochem. Soc. E **149**, 109 (2002)
20. M.C. Giménez, M.G. Del Pópolo, E.P.M. Leiva, Langmuir **18**, 9087 (2002)
21. M.C. Gimenez, E.V. Albano, J. Phys. Chem. C **111**, 1809 (2007)
22. L. Gammaitoni, P. Hänggi, P. Jung, F. Marchesoni, Eur. Phys. J. B **69**, 1 (2009)
23. R. Benzi, S. Sutera, A. Vulpiani, J. Phys. A **14**, L453 (1981)
24. C. Nicolis, G. Nicolis, Tellus **33**, 225 (1981)
25. P. Hänggi, ChemPhysChem **3**, 285 (2002)
26. Ding Hong-Bo, Xia Bao-Yun, Yin Chun-Sheng, Pan Zhong-Xiao, Electrochemistry **6**, 279 (2000)
27. P. Parmananda, G.J. Escalera Santos, M. Rivera, K. Showalter, Phys. Rev. E **71**, 031110 (2005)
28. M.C. Gimenez, J.A. Revelli, M.S. de la Lama, J.M. Lopez, H.S. Wio, Physica A **392**, 278 (2013)
29. M.C. Gimenez, J.A. Revelli, H.S. Wio, ICST Trans. Complex Systems **12**, e3 (2012)
30. M.P. Allen, D.J. Tildesley, *Computer Simulation of Liquids* (Oxford University Press, 1987)
31. N. Metropolis, A. Rosenbluth, M. Rosenbluth, A. Teller, E. Teller, J. Chem. Phys. **21**, 1087 (1953)
32. T.L. Hill, *An Introduction to Statistical Thermodynamics* (Dover publications, Inc., 1986)
33. S.W. Sides, P.A. Rikvold, M.A. Novotny, Phys. Rev. E **57**, 6512 (1998)
34. S.W. Sides, P.A. Rikvold, M.A. Novotny, Phys. Rev. Lett. **81**, 834 (1998)
35. G. Korniss, P.A. Rikvold, M.A. Novotny, Phys. Rev. E **66**, 056127 (2002)